Plasmonic Space Folding: Focusing Surface Plasmons *via* Negative Refraction in Complementary Media

Muamer Kadic,[†] Sebastien Guenneau,[†] Stefan Enoch,[†,*] and S. Anantha Ramakrishna[‡]

[†]Institut Fresnel, CNRS, Aix-Marseille Université, Campus Universitaire de Saint-Jérôme, 13013 Marseille, France and [‡]Department of Physics, Indian Institute of Technology, Kanpur 208016, India

ABSTRACT We extend designs of perfect lenses to the focusing of surface plasmon polaritons (SPPs) propagating at the interface between two anisotropic media of opposite permittivity sign. We identify the role played by the components of anisotropic and heterogeneous tensors of permittivity and permeability, deduced from a coordinate transformation, in the dispersion relation governing propagation of SPPs. We illustrate our theory with three-dimensional finite element computations for focusing of SPPs by perfect flat and cylindrical lenses. Finally, we propose a design of a flat SPP lens consisting of dielectric cylinders arranged in a periodic fashion (along a hexagonal array) on a metal plate.

KEYWORDS: transformation optics · surface plasmon polariton · metamaterial · flat lens

Subwavelength focusing and imaging of light using negative refractive index materials[1,2] is now a well-established phenomenon.[3,4] There has also been a growing interest in better controlling the passage of light, including invisibility to radiation using transformational optics, following the recent proposals by Pendry *et al.*[5] and Leonhardt.[6] Such singular invisibility cloaks are based upon the blowup of a point, which also finds interesting applications in inverse problems.[7] Importantly, the structure of transformed Maxwell's equations can be found in a classical textbook by Post[8] and can be deduced from the equations of general relativity,[9] the later allowing for the design of unconventional optical devices mimicking celestial bodies;[10] see also refs 11 and 12 for insightful reviews. Much of invisibility by cloaking is actually akin to the mirage effect:[13] for example, a point source located inside a cloak appears to radiate from a shifted location. Adopting this viewpoint, complementary media[4,14] within which focusing effects *via* negative refraction occur can be designed using geometric transforms by mapping the image plane back onto the source plane.[15,16] Such lenses were coined as Alice's mirrors in ref 17 since they exhibit certain antisymmetric features. These make also possible perfect and poor man's cylindrical lenses,[18−21] as well as generalized corner and checkerboard lenses.[4,22,23,25]

There are other types of electromagnetic waves also well worth controlling such as surface plasmon polaritons (SPPs), which allow for fascinating applications in the emerging field of nano-optics.[26,27] Back in 1998, Ebbesen *et al.*[28] established that resonant excitation of SPPs on a metal film perforated at subwavelength periodicities leads to unusually high transmission coefficients at certain frequencies. Pendry, Martin-Moreno, and Garcia-Vidal further showed in 2004 that one can view the localized resonances on structured, perfectly conducting surfaces as plasmonic excitations of a metamaterial surface.[29] Other plasmonic metamaterials include plasmonic shells with a suitable out-of-phase polarizability, in order to compensate the scattering from the knowledge of the electromagnetic parameters of the object to hide, and external cloaking, whereby a plasmonic resonance cancels the external field at the location of a given set of electric dipoles.[20,30−32] Imaging and focusing of surface plasmons on negative phase velocity interfaces of gold and polymer that are structured in layered, lens-like, or checkerboard fashions have also been experimentally studied by the group of Davis.[33] Agranovich *et al.*[34] have shown that one can obtain negative refraction for exciton-plasmon waves in organic and gyrotropic materials using a surface transition layer; see also the recent overview.[35]

In the present paper, we extend the design of transformation-based perfect lens to the focusing of surface plasmon polaritons. Our main contribution here is that we explain how one can manipulate SPPs such that the electromagnetic space where they live is folded back onto itself. In this manner, we extend the proposal of Pendry and

* Address correspondence to muamer.kadic@Fresnel.fr.

Received for review November 22, 2010 and accepted July 11, 2011.

Published online July 11, 2011
10.1021/nn201334m

Ramakrishna to build generalized lenses using the original concept of complementary media[4,14] to the context of surface plasmonic waves. This allows for instance the design of perfect corners, corner lenses, and the like,[4,22−25] using transformational plasmonics tools.[36−41] Importantly, the focusing of surface plasmons is amply demonstrated using full-wave computations involving materials such as gold with physical dispersions establishing the negative refraction of SPPs in a novel class of generalized plasmonic lenses.

This paper is organized in the following manner. In the next section, the ideas of transformational optics and optical space folding are briefly discussed and exemplified. These ideas are applied in Section 3 to generate generalized lenses for SPPs in rectangular coordinates and in Section 4 to generate lenses with curved surfaces in cylindrical coordinates. In Section 5, the design of a flat SPP lens using a dielectric photonic crystal is demonstrated, and we conclude in the last section with a summary of the main results.

TRANSFORMATIONAL OPTICS VERSUS OPTICAL SPACE FOLDING

Theoretically, perfect lenses can be designed using the techniques of transformation optics, whereby an unphysical solution in a folded geometry (a given region of optical space that is mapped onto itself) is turned into a physical solution in unfolded geometry (a metamaterial described by tensors of permittivity and permeability with sign-shifted coefficients). Let us consider the simple case of a cylindrical perfect lens i.e. a disk of radius R_1 surrounded by an annulus $R_1 \leq r \leq R_2$ and the piecewise continuous map:

$$\begin{cases} r' = f_1(r) & \text{in the core} \\ r' = f_2(r) & \text{in the shell} \\ r' = r\ pt & \text{elsewhere} \end{cases}$$

where $f_1(R_1) = f_2(R_1)$ and $f_2(R_2) = R_2$. We show in Figure 1a an example of such a mapping and in Figure 1b a typical range of values for the corresponding refractive index. A line source placed in the neighborhood of the cylindrical perfect lens (see Figure 1c) gives rise to two images: one image appears inside the negatively refracting coating and a second one inside the inner disk in accordance with negative refraction. We note that the wavelength shrinks inside the lens: the image is a demagnified copy of the source. If we now launch a plane wave on the cylindrical perfect lens (see Figure 1d), some anomalous resonances occur on the inner and outer boundaries of the lens, and this could be utilized to cloak a set of dipoles outside the lens.[21]

This technique allows us to transform many known situations in simple geometries into unknown solutions in more complicated geometries. With only some occasional exceptions, this technique usually results in the requirement of inhomogenous and anisotropic materials in the physical unfolded geometry. Essentially, all the deformation of space implied in the geometric transformation are piled onto the physical responses of the materials. Generating such situations is physically possible using present day metamaterials, although it could be very difficult.

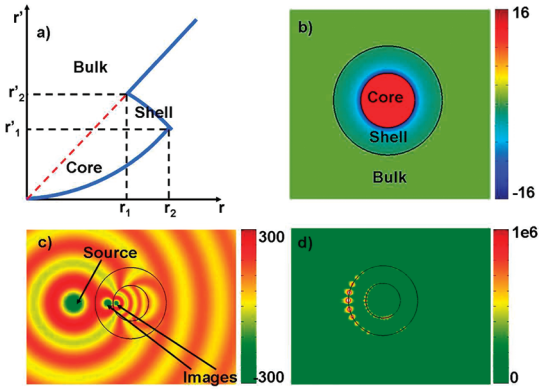

Figure 1. Focusing *via* optical space folding: (a) Sketch of the unfolding map where *r* and *r'* are the radial coordinates in folded and unfolded geometries. (b) Typical distribution of the permittivity in the perfect lens. (c) Two-dimensional plot of the real part of the longitudinal magnetic field [A/m] for an electric line source inside the core. (d) Magnitude of the magnetic field [A/m] for an incident plane wave.

TRANSFORMATIONAL PLASMONICS AND GENERALIZED PERFECT LENSES IN CARTESIAN COORDINATES FOR SPPS

We will now consider how the generalized perfect lens theorem[14] can be utilized to envisage perfect focusing of surface plasmons. The techniques of transformational optics are then used to generate physically realizable plasmonic superlenses in rectangular geometries.

Let us consider two semi-infinite regions separated by a plane interface at $x_2 = 0$. We can map these two isotropic homogeneous media on two metamaterials described by anisotropic heterogeneous matrices of permittivity and permeability given by[13]

$$\varepsilon' = \varepsilon \mathbf{T}^{-1}, \text{and } \mu' = \mu \mathbf{T}^{-1} \qquad (1)$$

where $\mathbf{T} = \mathbf{J}^T\mathbf{J}/\det(\mathbf{J})$ is the transformation matrix constructed using the Jacobian associated with the change of coordinates. The original perfect lens presupposed a slab of material with $\varepsilon = -1$ and $\mu = -1$. Let us now derive this result using the powerful tool of transformational plasmonics.[36] In order to design generalized lenses for surface plasmon polaritons, we want to fold the plasmonic space back onto itself, and this leads to negative coefficients within the permittivity and permeability matrices. The coordinate transformation is given by

$$\begin{aligned} x'_1 &= x_1 \\ x'_2 &= x_2 \\ x'_3 &= x_3 - d, \text{ if } x'_3 < d/2, \\ &\quad \text{or } -x_3 \text{ if } -d/2 < x_3 < d/2, \\ &\quad \text{or } x_3 + d \text{ if } d/2 < x_3 \end{aligned}$$

where d is the thickness of the generalized lens. The above coordinate transformation leads to the identity for

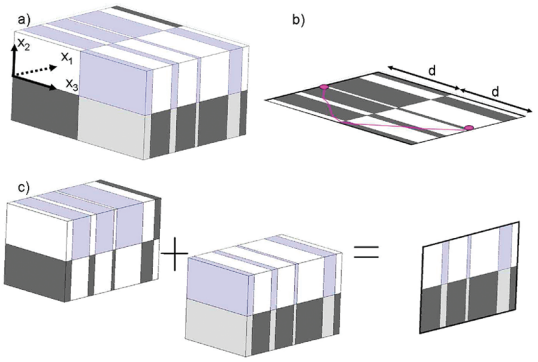

Figure 2. Principle of plasmonic space folding within complementary media. (a) An alternation of positively and negatively refracting index media in all three space dimensions cancels the plasmonic path (note that the bottom part (in gray color) is filled with Drude complementary media). (b) Typical propagation path for a SPP at the $x_2 = 0$ interface. (c) Underlying space folding mechanism whereby the combination of two regions of complementary media is equivalent to a heterogeneous interface.

the transformation matrix **T** outside the lens, whereas inside the lens, *i.e.*, for $-d/2 < x'_3 < d/2$, $\partial x_3/\partial x'_3 = -1$, it flips the sign of T_{33}, so that the material properties differ from free space only for points along the $x_3 = x'_3$ direction. This analysis demonstrates that SPP focusing will always occur irrespective of the medium in which the lens is embedded. This is true for any medium that is mirror antisymmetric about a vertical plane.

In the case of anisotropic $\underline{\varepsilon'^i_j}$ and $\underline{\mu'^i_j}$, the transformed media are now characterized in the region $-d < x_3 < 0$ by

$$\underline{\varepsilon'^i_j} = \varepsilon_j(-1)\begin{pmatrix}1&0&0\\0&1&0\\0&0&-1\end{pmatrix}\begin{pmatrix}\varepsilon^i_{11}&\varepsilon^i_{12}&\varepsilon^i_{13}\\\varepsilon^i_{21}&\varepsilon^i_{22}&\varepsilon^i_{23}\\\varepsilon^i_{31}&\varepsilon^i_{32}&\varepsilon^i_{33}\end{pmatrix}\begin{pmatrix}1&0&0\\0&1&0\\0&0&-1\end{pmatrix}$$
$$\underline{\mu'^i_j} = (-1)\begin{pmatrix}1&0&0\\0&1&0\\0&0&-1\end{pmatrix}\begin{pmatrix}\mu^i_{11}&\mu^i_{12}&\mu^i_{13}\\\mu^i_{21}&\mu^i_{22}&\mu^i_{23}\\\mu^i_{31}&\mu^i_{32}&\mu^i_{33}\end{pmatrix}\begin{pmatrix}1&0&0\\0&1&0\\0&0&-1\end{pmatrix} \quad (2)$$

We note that there is no change in the impedance of the media, since the permittivity and permeability undergo the same geometric transformation: the perfect lens is impedance-matched with its surrounding medium (air, say) so that no reflection will occur at its interfaces.

Then the resulting complementary medium (see Figure 2) is given by

$$\underline{\varepsilon'^i_j} = \varepsilon_j\begin{pmatrix}-\varepsilon^i_{11}&-\varepsilon^i_{12}&+\varepsilon^i_{13}\\-\varepsilon^i_{21}&-\varepsilon^i_{22}&+\varepsilon^i_{23}\\+\varepsilon^i_{31}&+\varepsilon^i_{32}&-\varepsilon^i_{33}\end{pmatrix},$$
$$\underline{\mu'^i_j} = \begin{pmatrix}-\mu^i_{11}&-\mu^i_{12}&+\mu^i_{13}\\-\mu^i_{21}&-\mu^i_{22}&+\mu^i_{23}\\+\mu^i_{31}&+\mu^i_{32}&-\mu^i_{33}\end{pmatrix},$$
$$0 < x_3 < d \quad (3)$$

where $\varepsilon_1 = 1$ and ε_2 are as in eq 4, and $j = 1$ for $x_2 > 0$ and $j = 2$ for $x < 0$. This is a generalization to transformational plasmonics of the result first derived in ref 4 and retrieved again using group theory (symmetries of

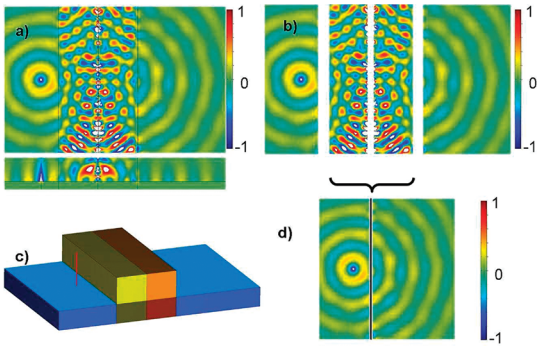

Figure 3. SPP focusing in a checkerboard lens at 700 nm: (a) top and side views of the computed field for a SPP line source; (c) four complementary media: $\varepsilon^1_1 = \mu^1_1 = 2$ in yellow block, $\varepsilon^1_2 = \mu^1_2 = -2$ in orange block with their Drude metal counterparts $\varepsilon^2_1 = \mu^2_1 = 2(1 - (\omega_p{}^2)/(\omega^2 + i\gamma\omega))$ in dark yellow block, $\varepsilon^2_2 = \mu^2_2 = -2(1 - (\omega_p{}^2)/(\omega^2 + i\gamma\omega))$ in red block underneath. (b) The middle regions cancel each other, leading to (d).

Maxwell's equations) in ref 23. The entries in $\underline{\varepsilon^i_j}$ and $\underline{\mu^i_j}$ can also be spatially varying along x_1 and x_2. This covers the case of perfect corner reflectors of $2n$-fold skew symmetry, and we are therefore ensured of the cancellation of the plasmonic path. It is worth noting that the generalized lens theorem was also applied to infinite checkerboards of skew symmetry in refs 23 and 25.

For the sake of concreteness, we will assume materials with physical dispersive forms of a Drude metal. The upper region ($x_2 > 0$) is considered to be vacuum or air, *i.e.*, with relative permittivity $\varepsilon_1 = 1$ (respectively relative permeability $\mu_1 = 1$), while the lower region ($x_2 < 0$) is filled with a Drude metal *i.e.*, with relative permittivity

$$\varepsilon_2 = 1 - \frac{\omega_p{}^2}{\omega^2 + i\gamma\omega} \quad (4)$$

(respectively relative permeability $\mu_2 = 1$): here, some gold with the plasma frequency ($\omega_p = 2175$ THz) and characteristic collision frequency ($\gamma = 4.35$ THz). For the plasmonic case of focusing, we can define two complementary media above the metal surface and two complementary media within the metal as

$$\varepsilon^1_j = +\varepsilon_j\varepsilon(x_1, x_2), \mu^1_j = +\mu(x_1, x_2), \quad -d < x_3 < 0$$
$$\varepsilon^2_j = -\varepsilon_j\varepsilon(x_1, x_2), \mu^2_j = -\mu(x_1, x_2), 0 < x_3 < d$$

Case $j = 1$ corresponds to the top region, $0 < x_2 < +\infty$, while case $j = 2$ corresponds to the bottom region, $-\infty < x_2 < 0$, with $\varepsilon_1 = 1$ and ε_2 as in eq 4.

We report in Figure 3 some finite element computations showing focusing of a SPP at a wavelength of 700 nm for two such complementary media, *i.e.*, a checkerboard lens for the special case $\varepsilon(x_1,x_2) = \mu(x_1,x_2) = 2$. The cancellation of *plasmonic* space is noted.

We further show in Figure 4 a focusing effect through a plasmonic flat lens with $\varepsilon(x_1,x_2) = \mu(x_1,x_2) = 1$. The source and the perfect images indeed satisfy the inverted Snell–Descartes laws of negative refraction, as shown for a SPP beam incident upon the lens at an angle of 45°. Let us emphasize here that in our numerical

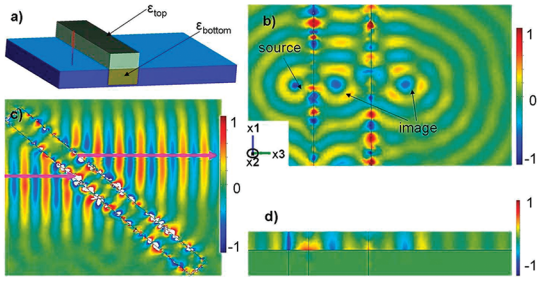

Figure 4. Perfect plasmonic lens *via* negative refraction at 700 nm: (a) the medium $\varepsilon_1^1 = \mu_1^1 = -1$ in the yellow block and its Drude metal counterpart underneath $\varepsilon_1^2 = -(1 - (\omega_p{}^2)/(\omega^2 + i\gamma\omega))$, $\mu_1^2 = -1$; (b) top and side views of the computed field for a SPP line source; (c) negatively refracted SPP beam making an angle of 45° with the lens. White regions in the plot of panel (c) correspond to large values of the field outside the color scale.

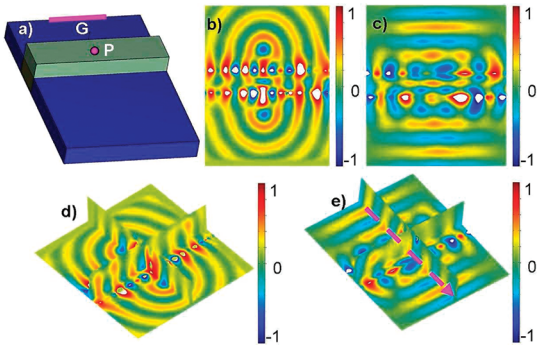

Figure 5. Compact anisotropic plasmonic lens at 700 nm. (a) 3D view of a three-dimensional anisotropic perfect lens. Two cases have been studied: a Gaussian beam of waste 2100 nm on normal incidence launched from the line G and a line source at point P. (b) Magnetic field phase for a line source placed at the point P. (c) Magnetic field phase for a Gaussian beam launched from the line G. (d) 3D view of (b). (e) 3D view of (c) with the arrow pointing toward the direction of propagation. White regions in the plots correspond to large values of the field outside the color scale.

implementation we make use of finite edge elements that are nothing but discrete Whitney differential forms and behave nicely under pull-back transforms.[42] Thus, in what follows, we always map the destination domain onto the original one (so we consider the inverse transforms).

We then extend the dispersion relation for a surface plasmon at the interface between a transformed medium and a transformed metal[36] to the case where we have four media described by diagonal tensors of relative permittivity and permeability: $\underline{\varepsilon_j^i} = \mathrm{diag}(\varepsilon_{11j}^i, \varepsilon_{22j}^i, \varepsilon_{33j}^i)$ and $\underline{\mu_j^i} = \mathrm{diag}(\mu_{11j}^i, \mu_{22j}^i, \mu_{33j}^i)$ with $j = 1$ when $x_2 > 0$ and $j = 2$ when $x_2 < 0$; see Figure 2a. The SPP propagating at the metal surface has a wavenumber satisfying

$$k_3^i = \frac{\omega}{c}\sqrt{\frac{\varepsilon_{33,2}^i \varepsilon_{33,1}^i (\mu_{22,2}^i \varepsilon_{11,1}^i - \mu_{22,1}^i \varepsilon_{11,2}^i)}{\varepsilon_{11,1}^i \varepsilon_{33,1}^i - \varepsilon_{11,2}^i \varepsilon_{33,2}^i}} \quad (5)$$

where $i = 1, 2$ denotes the ith transformed medium and its Drude metal counterpart. This formula also characterizes the wavenumber of an SPP propagating at a multilayered metal surface, whereby the number i of complementary regions is constrained only by the overall propagation length of the SPP. It should be noted that the condition for existence of a SPP at the interface between two anisotropic media (see ref 37),

$$\frac{k_2^1}{\varepsilon_{11,1}} + \frac{k_2^2}{\varepsilon_{11,2}} = 0 \quad (6)$$

is always met, and this ensures the SPP does not scatter from the interface.

Following the work by Shen *et al.*[43] on two-dimensional anisotropic perfect lenses, we report in Figure 5 some computations for a beam of SPP (Gaussian beam) incident from the left on such a lens in the three-dimensional transformational plasmonic setting. Above the metal interface, the transformed medium is described by

$$\underline{\varepsilon_1} = \mathrm{diag}(\varepsilon_{11,1}, \varepsilon_{22,1}, \varepsilon_{33,1}) = (-2 + 0.001i,\ -2 + 0.001i,\ -0.5 + 0.001i)$$

and

$$\underline{\mu_1} = \mathrm{diag}(\mu_{11,1}, \mu_{22,1}, \mu_{33,1}) = (-2 + 0.001i,\ -2 + 0.001i,\ -0.5 + 0.001i)$$

for the bottom layer, and the transformed metal is described by

$$\underline{\varepsilon_2} = \mathrm{diag}(\varepsilon_{11,2}, \varepsilon_{22,2}, \varepsilon_{33,2}) = \varepsilon_2(-2 + 0.001i,\ -2 + 0.001i,\ -0.5 + 0.001i)$$

and

$$\underline{\mu_2} = \mathrm{diag}(\mu_{11,2}, \mu_{22,2}, \mu_{33,2}) = (-2 + 0.001i,\ -2 + 0.001i,\ -0.5 + 0.001i)$$

which is a particular case of eq 3. In panels (b) and (d) of Figure 5, we place a line source within the slab lens (shown by point P in panel (a)), and we observe two perfect images on either side of the anisotropic lens, in accordance with the perfect lens theorem. We note that on the vertical sides of this lens, the following condition is met:

$$\frac{\varepsilon_{11,j}}{\mu_{22,j}} = \frac{\varepsilon_j}{\mu_j},\ \varepsilon_{11,j}\varepsilon_{33,j} = (\varepsilon_j)^2,$$
$$\frac{\mu_{11,j}}{\varepsilon_{22,j}} = \frac{\mu_j}{\varepsilon_j},\ \mu_{11,j}\mu_{33,j} = (\mu_j)^2 \quad (7)$$

where $\varepsilon_1 = \mu_1 = 1$ describes the ambient medium above the surface (air), ε_2 is as in eq 4, and $\mu_2 = 1$. Hence, the slab lens is perfectly matched to the surrounding medium. We have numerically checked this fact by sending a Gaussian SPP beam with a waist of $3\lambda = 2100$ nm on this rather unusual lens. The wavefront shrinks within the lens, but forward and backward scatterings do not sense the presence of the lens: the lens is indeed perfectly impedance matched for any SPP propagating on the metal surface.

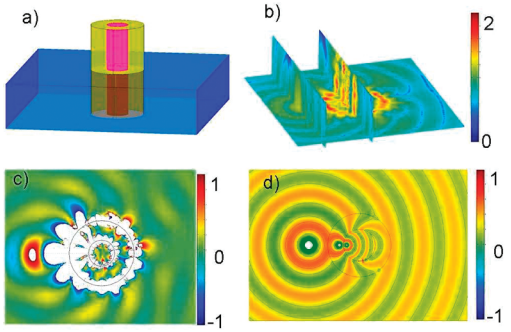

Figure 6. Focusing through a cylindrical plasmonic lens for a SPP line source at wavelength 700 nm. (a) Schematic diagram of the cylindrical lens. The pink region is filled with spatially varying permittivity $(R_2/R_1)^4$ above and its Drude metal counterpart below, $\varepsilon_2(R_2/R_1)^4$; the gold region is filled with negative permittivity $-R_2^2/r^2$ and negative permittivity -1 above and its Drude metal counterpart below (with a permittivity $-\varepsilon_2 R_2^2/r^2$ and negative permittivity -1). (b) 3D plot of $\log(1+|H|)$, where H is the magnetic field. (c) 2D plot of the magnetic field. (d) 2D computation for TE waves (with parameters of the top regions of (a). White regions in the 2D plots (c) and (d) correspond to large values of the field outside the color scale. The metal permitivitty is taken from the Drude model: $\varepsilon_2 = (1-(\omega_p{}^2)/(\omega^2+i\gamma\omega))$ and $r^2 = x^2+y^2$.

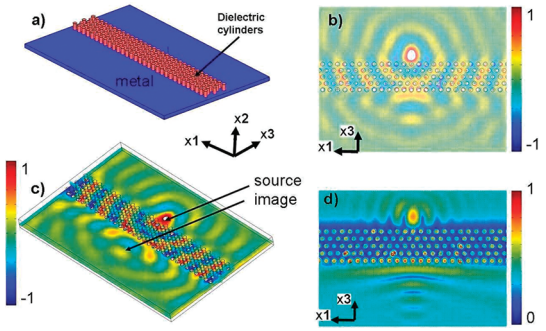

Figure 7. Focusing through a plasmonic lens for a SPP line source at wavelength $\lambda = 700$ nm. (a) Schematic diagram of the flat SPP lens with a hexagonal lattice of dielectric cylinders (permittivity $\varepsilon_1{}^* = 13$, diameter $d = 107$ nm, and height $h = 700$ nm) with center-to-center spacing of $a = 180$ nm, on a metal plate (Drude model with permittivity $\varepsilon_2 = (1-(\omega_p{}^2)/(\omega^2+i\gamma\omega))$. (b) 2D plot of the phase of the magnetic field. (c) 3D plot of the phase of the magnetic field. (d) 2D plot of the magnitude of the magnetic field.

TRANSFORMATIONAL PLASMONICS AND GENERALIZED PERFECT LENSES IN CYLINDRICAL COORDINATES FOR SPPS

Building on the previous perfect lens theory,[14] we can use geometric transformations to bend the shape of the perfect lens into other geometries such as two concentric cylinders; see Figure 6a. The objective is to follow Pendry's proposal of a magnifying glass, in which case the lens must be curved. This is because a flat lens invariant along the parallel directions preserves the parallel wavevectors and cannot affect the distribution of wavevectors from the source. A curved surface, in contrast, breaks this transverse invariance and can result in the magnification or demagnification of the images. The conformal transformation $z' = \ln z$, where $z = x + iy$, is known to preserve the solutions of Laplace's equation and leaves the values of ε and μ unchanged.[4] However, when one departs from the static case, the previous geometric transformation of the full Maxwell's equations leads to anisotropic heterogeneous permittivity and permeability tensors.

Following the same algorithm as in the previous section, we find that a possible design for a cylindrical perfect lens for SPPs (avoiding spatially varying media outside the lens) is given by

$$\begin{aligned} \varepsilon_j^1 &= \varepsilon_j(R_2/R_1)^4,\ \mu_j^2 = 1,\ r \le R_1 \\ \varepsilon_j^2 &= -\varepsilon_j R_2^2/r^2,\ \mu_j^2 = -1,\ R_1 \le r \le R_2 \end{aligned} \quad (8)$$

with $j = 1$ for $x_2 > 0$, $j = 2$ for $x_2 < 0$, and $\varepsilon_1 = 1$ and ε_2 as in eq 4.

We show in panels (b) and (d) of Figure 6 some 3D finite element computations for a SPP line source at a wavelength of 700 nm, located inside the central region of the cylindrical lens. We also depict in panel (c) a 2D numerical simulation for comparison with the case of transverse electric waves (whereby $\varepsilon_1 = \varepsilon_2 = 1$). We note that in this configuration the image is indeed magnified.

PROPOSAL OF A FLAT SPP LENS WITH A DIELECTRIC PHOTONIC CRYSTAL

The transformational plasmonics designs discussed above still need to be implemented with structured metasurfaces. In order to do so, we looked at the vast literature on dielectric photonic crystal lenses *via* all-angle-negative refraction (AANR) (see, *e.g.*, ref 44 and 45) as well as on focusing effects using the dispersion relation of metals.[33,46,47] As far as we know, no structured dielectric device has been proposed yet in order to get the AANR effect for surface plasmon polaritons. The advantage of this approach is to allow for a large enough amplitude of the plasmonic field to be transmitted through the structured lens, as the absorption in a dielectric is less than in metal. We first designed an AANR lens with optimized parameters using a two-dimensional model with effective parameters (following the approach of ref 40, the effective permittivity of dielectric cylinders was taken to be $\varepsilon_1\varepsilon_2/(\varepsilon_1+\varepsilon_2)$, where ε_1 is the permittivity of the dielectric cylinder above the Drude metal of permittivity ε_2). This means we consider a photonic crystal with two phases of permittivity depending upon the SPP wavelength. The much reduced computing time compared to full-wave three-dimensional computations enables us to apply a simple optimization algorithm whereby the objective function is the magnitude of the field at the theoretical position for the image point. We show in Figure 7 the plot of the longitudinal field for the optimized set of parameters (when the image amplitude is the largest one). We then used the optimized parameter $\varepsilon_1{}^*$ in the dielectric cylinders above the metal, which turns out to be $\varepsilon_1{}^* = 13$. Such a permittivity can be found in

semiconductors in the visible range of frequencies. We report in Figure 7 the three-dimensional computations for an SPP wavelength of 800 nm. Importantly, it is possible to further enhance the transmitted field through the photonic crystal by adding a little bit of gain in the structured lens. We believe the design that we propose could be implemented in the near future in an experimental setup such as discussed in ref 37.

CONCLUSION

In conclusion, we have studied analytically and numerically the extension of optical space folding to the area of plasmonics and surface plasmon focusing. This requires in general anisotropic heterogeneous complementary media deduced from geometric transformations. Focusing of SPPs resulting in a markedly enhanced control of their wave trajectories and imaging of sources by SPPs have been demonstrated. Importantly, our analysis applies *mutatis mutandis* for an s-polarized SPP (interchanging the roles of permittivity and permeability). For illustrative purposes, checkerboard and cylindrical designs of SPP lenses have been proposed and implemented in the finite element commercial package COMSOL. The feasability of our transformational approach has been validated with a structured design of a negative refraction.

METHODS

The numerical simulations of this paper have been performed using the commercial finite element package COMSOL, which solves the three-dimensional Maxwell system with scattering boundary conditions and perfectly matched layers (PMLs). This ensures we have reflectionless interfaces between the region of interest (containing the metamaterial under study) and surrounding regions filled with anisotropic heterogeneous and lossy media damping the outgoing waves (PMLs). The direct solver PARDISO was used, and typically one million tetrahedral elements were needed in order to achieve full convergence of the numerical solution (the maximum element size of our mesh was set to $\lambda/8$, with λ the working wavelength).

Acknowledgment. The authors are grateful for insightful comments by Mr. G. Dupont and Prof. R. Quidant. M.K. acknowledges funding from the French Ministry of Higher-Education and Research. S.G., S.A.R., and S.E. are thankful for funding to the Indo-French Centre for the Promotion of Advanced Research, New Delhi, under project no. IFCPAR/3804-2.

REFERENCES AND NOTES

1. Veselago, V. G. The Electrodynamics of Substances with Simultaneously Negative Values of Permittivity and Permeability. *Soviet Phys. Usp.* **1968**, *10*, 509–514.
2. Ramakrishna, S. A.; Grzegorczyk, T. M. *Physics and Applications of Negative Refractive Index Materials*; CRC Press, 2008.
3. Pendry, J. B. Negative Refraction Makes a Perfect Lens. *Phys. Rev. Lett.* **2000**, *85*, 3966–3969.
4. Pendry, J. B.; Ramakrishna, S. A. Focusing Light with Negative Refractive Index. *J. Phys.: Condens. Matter* **2003**, *15*, 6345–6364.
5. Pendry, J. B.; Schurig, D.; Smith, D. R. Controlling Electromagnetic Fields. *Science* **2006**, *312*, 1780–1782.
6. Leonhardt, U. Optical Conformal Mapping. *Science* **2006**, *312*, 1777–1779.
7. Greenleaf, A.; Lassas, M.; Uhlmann, G. On Nonuniqueness for Calderon's Inverse Problem. *Math. Res. Lett.* **2003**, *10*, 685–93.
8. Post, E. G. *Formal Structure of Electromagnetics: General Covariance and Electromagnetics*, Interscience Publishers, 1962.
9. Leonhardt, U.; Philbin, T. G. General Relativity in Electrical Engineering. *New J. Phys.* **2006**, *8*, 247.
10. Genov, D. A.; Zhang, S.; Zhang, W. Mimicking Celestial Mechanics in Metamaterials. *Nat. Phys.* **2009**, *5*, 687–692.
11. Chen, H.; Chan, C. T.; Sheng, P. Transformation Optics and Metamaterials. *Nat. Mater.* **2010**, 387–396.
12. Kildishev, A. V.; Cai, W.; Chettiar, U. K.; Shalaev, V. M. Transformation Optics: Approaching Broadband Electromagnetic Cloaking. *New J. Physics* **2008**, *10*, 115029.
13. Zolla, F.; Guenneau, S.; Nicolet, A.; Pendry, J. B. Electromagnetic Analysis of Cylindrical Invisibility Cloaks and the Mirage Effect. *Opt. Lett.* **2007**, *32*, 1069–1071.
14. Pendry, J. B.; Ramakrishna, S. A. Near Field Lenses in Two Dimensions. *J. Phys.: Condens. Matter* **2002**, *14*, 8463–8479.
15. Leonhardt, U.; Philbin, T. G. Transformation Optics and the Geometry of Light. *Prog. Opt.* **2009**, *53*, 69–152.
16. Guenneau, S.; Ramakrishna, S. A. Negative Refractive Index, Perfect Lenses and Checkerboards: Trapping and Imaging Effects in Folded Optical Spaces. *C. R. Phys.* **2009**, *10*, 352–378.
17. Maystre, D.; Enoch, S. Perfect Lenses Made with Left Handed Materials: Alice's Mirror. *J. Opt. Soc. Am. A* **2004**, *21*, 122–131.
18. Pendry, J. B. Perfect Cylindrical Lenses. *Opt. Express* **2003**, *11*, 755–760.
19. Nicorovici, N. A.; McPhedran, R. C.; Milton, G. W. Transport Properties of a Three-phase Composite Material: the Square Array of Coated Cylinders. *Proc. R. Soc. A* **1993**, *442*, 599–620.
20. Nicorovici, N. A.; McPhedran, R. C.; Milton, G. W. Optical and Dielectric Properties of Partially Resonant Composites. *Phys. Rev. B* **1994**, *49*, 8479–8482.
21. Nicorovici, N. A.; Milton, G. W. On the Cloaking Effects Associated with Anomalous Localised Resonance. *Proc. R. Soc. London A* **2006**, *462*, 3027–3059.
22. Guenneau, S.; Gralak, B.; Pendry, J. B. Perfect Corner Reflector. *Opt. Lett.* **2005**, *30*, 1204–1206.
23. Guenneau, S.; Vutha, A. C.; Ramakrishna, S. A. Negative Refraction in 2D Checkerboards Related by Mirror antisymmetry and 3D Corner Lenses. *New J. Phys.* **2005**, *7*, 164.
24. He, S. L.; Jin, Y.; Ruan, Z. C.; Kuang, J. G. On Subwavelength and Open Resonators Involving Metamaterials of Negative Refraction Index. *New J. Phys.* **2005**, *7*, 210.
25. Chakrabarti, S.; Ramakrishna, S. A.; Guenneau, S. Finite Checkerboards of Dissipative Negative Refractive Index. *Opt. Express* **2006**, *14*, 12950–12957.
26. Zayats, A. V.; Smolyaninov, I. I.; Maradudin, A. A. Nano-optics of Surface Plasmon Polaritons. *Phys. Rep.* **2005**, *408*, 131–314.
27. Maier, S. *Plasmonics: Fundamentals and Applications*; Springer Verlag, 2007.
28. Ebbesen, T. W.; Lezec, H. Y.; Ghaemi, H. F.; Thio, T.; Woff, P. A. Extraordinary Optical Transmission through Subwavelength Hole Arrays. *Nature* **1998**, *391*, 667–669.
29. Pendry, J. B.; Martin-Moreno, L.; Garcia-Vidal, F. J. Mimicking Surface Plasmons with Structured Surfaces. *Science* **2004**, *305*, 847–848.
30. Alu, A.; Engheta, N. Achieving Transparency with Plasmonic and Metamaterial Coatings. *Phys. Rev. E* **2005**, *72*, 016623.
31. Garcia de Abajo, F. J.; Gomez-Santos, G.; Blanco, L. A.; Borisov, A. G.; Shabanov, S. V. Tunneling Mechanism of

Light Transmission Through Metallic Films. *Phys. Rev. Lett.* **2005**, *95*, 067403.
32. Baumeier, B.; Leskova, T. A.; Maradudin, A. A. Cloaking from Surface Plasmon Polaritons by a Circular Array of Point Scatterers. *Phys. Rev. Lett.* **2009**, *103*, 246809.
33. Smolyaninov, I. I.; Hung, Y.-J.; Davis, C. C. Imaging and Focusing Properties of Plasmonic Metamaterial Devices. *Phys. Rev. B* **2007**, *76*, 205424.
34. Agranovich, V. M.; Shen, R. Y.; Baughman, R. H.; Zakhidov, A. A. Optical Bulk and Surface Waves with Negative Refraction. *J. Lumin.* **2004**, *110*, 167–173.
35. Fu, Y.; Zhou, X. Plasmonic Lenses: A Review. *Plasmonics* **2010**, *1*, 24.
36. Kadic, M.; Guenneau, S.; Enoch, S. Transformational Plasmonics: Cloak, Concentrator and Rotator for SPPs. *Opt. Express* **2010**, *18*, 12027–12032.
37. Renger, J.; Kadic, M.; Dupont, G.; Acimovic, S.; Guenneau, S.; Quidant, R.; Enoch, S. Hidden Progress: Broadband Plasmonic Invisibility. *Opt. Express* **2010**, *18*, 15757–15768.
38. Liu, Y.; Zentgraf, T.; Bartal, G.; Zhang, X. Transformational Plasmon Optics. *Nano Lett.* **2010**, *10*, 1991–1997.
39. Huidobro, P. A.; Nesterov, M. L.; Martin-Moreno, L.; Garcia-Vidal, F. J. Transformation Optics for Plasmonics. *Nano Lett.* **2010**, *10*, 1985–1990.
40. Aubry, A.; Lei, D. Y.; Maier, S. A. Broadband Plasmonic Device Concentrating the Energy at the Nanoscale: the Crescent-shaped Cylinder. *Phys. Rev. B* **2010**, *82*, 125430.
41. Aubry, A.; Lei, D. Y.; Maier, S. A.; Pendry, J. B. Interaction Between Plasmonic Nanoparticles Revisited with Transformation Optics. *Phys. Rev. Lett.* **2010**, *105*, 233901.
42. Bossavit, A. *Computational Electromagnetism*; Academic Press: Boston, 1998.
43. Shen, N. H.; Foteinopoulou, S.; Kafesaki, M.; Koschny, Th.; Ozbay, E.; Economou, E. N.; Soukoulis, C. N. Compact Planar Far-field Superlens Based on Anisotropic Left-handed Metamaterials. *Phys. Rev. B* **2009**, *80*, 115123.
44. Gralak, B.; Enoch, S.; Tayeb, G. Anomalous Refractive Properties of Photonic Crystals. *J. Opt. Soc. Am. A* **2000**, *17*, 1012–1020.
45. Luo, C.; Johnson, S. G.; Joannopoulos, J. D.; Pendry, J. B. Three-dimensional Light Focusing in Inverse Opal Photonic Crystals. *Phys. Rev. B* **2002**, *65*, 201104.
46. Fang, N.; Lee, H.; Sun, C.; Zhang, X. Sub-diffraction-limited Optical Imaging with a Silver Superlens. *Science* **2005**, *308*, 534–537.
47. Shin, H.; Fan, S. All-angle Negative Refraction for Surface Plasmon Waves Using a Metal-dielectric-metal Structure. *Phys. Rev. Lett.* **2006**, *96*, 073907.